Experimental High-Resolution Winter Seasonal Climate Reforecasts for Florida

AMIT BHARDWAJ,[a,b] VASUBANDHU MISRA,[a,b,c] BEN KIRTMAN,[d] TIRUSEW ASEFA,[e,f] CAROLINA MARAN,[g] KEVIN MORRIS,[h] ED CARTER,[i] CHRISTOPHER MARTINEZ,[j] AND DANIEL ROBERTS[k]

[a] *Center for Ocean–Atmospheric Prediction Studies, Florida State University, Tallahassee, Florida*
[b] *Florida Climate Institute, Florida State University, Tallahassee, Florida*
[c] *Department of Earth, Ocean, and Atmospheric Science, Florida State University, Tallahassee, Florida*
[d] *Rosenstiel School of Marine and Atmospheric Sciences, University of Miami, Miami, Florida*
[e] *Planning and Systems Decision Support, Tampa Bay Water, Clearwater, Florida*
[f] *Patel College of Global Sustainability, University of South Florida, Tampa, Florida*
[g] *South Florida Water Management District, Broward County, Florida*
[h] *Manatee County Utilities, Bradenton, Florida*
[i] *St. Johns River Water Management District, Jacksonville, Florida*
[j] *Department of Agricultural and Biological Engineering, Institute of Food and Agricultural Sciences, University of Florida, Gainesville, Florida*
[k] *Peace River Manasota Regional Water Supply Authority, Lakewood Ranch, Florida*

(Manuscript received 11 December 2020, in final form 10 March 2021)

ABSTRACT: We present here the analysis of 20 years of high-resolution experimental winter seasonal climate reforecasts for Florida (CLIFF). These winter seasonal reforecasts were dynamically downscaled by a regional atmospheric model at 10-km grid spacing from a global model run at T62 spectral resolution (~210-km grid spacing at the equator) forced with sea surface temperatures (SST) obtained from one of the global models in the North American Multimodel Ensemble (NMME). CLIFF was designed in consultation with water managers (in utilities and public water supply) in Florida targeting its five water management districts, including two smaller watersheds of two specific stakeholders in central Florida that manage the public water supply. This enterprise was undertaken in an attempt to meet the climate forecast needs of water management in Florida. CLIFF has 30 ensemble members per season generated by changes to the physics and the lateral boundary conditions of the regional atmospheric model. Both deterministic and probabilistic skill measures of the seasonal precipitation at the zero-month lead for November–December–January (NDJ) and one-month lead for December–January–February (DJF) show that CLIFF has higher seasonal prediction skill than persistence. The results of the seasonal prediction skill of land surface temperature are more sobering than precipitation, although, in many instances, it is still better than the persistence skill.

KEYWORDS: Ensembles; Probability forecasts/models/distribution; Seasonal forecasting; Climate models; Seasonal variability

1. Introduction

This paper reports on an exclusive set of seasonal reforecasts done over Florida in an attempt to meet the needs of the water resource managers in utilities and public water supply across Florida. Florida is uniquely divided into five water management districts (Fig. 1a) that have the core mission of monitoring and assessing water supply, water quality, operating and managing flood protection and floodplain management, evaluate, and protect natural systems by regulating freshwater flows. These water managers have interacted with the authors of the paper through the Florida Water and Climate Alliance (FloridaWCA; http://www.floridawca.org), where a desire to have customized seasonal predictions was expressed. The five water management districts, in addition to two wholesale water suppliers in Central Florida: Tampa Bay Water (TBW) and Peace River Manasota Regional Water Supply Authority (PRM) are part of FloridaWCA. These organizations would benefit from a customized seasonal prediction over their regions in order to manage and regulate freshwater resources to meet their needs. As noted in Misra et al. (2019), the spatial resolution of the global climate models (~100-km grid spacing) are rather inadequate to resolve their watersheds (e.g., PRM, TBW in Fig. 1a), coastlines of Florida (e.g., Fig. 1b) and even some weather events (e.g., sea breeze) that aggregate to cause significant seasonal climate anomalies (Bastola and Misra 2013; Shi and Misra 2020).

Despite publicly available hydroclimatic forecasts, for example, from NOAA Climate Prediction Center (CPC) or the International Research Institute for Climate and Society, water resource managers are not always receptive to using them (Dow et al. 2007; Lemos 2008; Bolson et al. 2013; Whateley et al. 2015; Misra et al. 2021). Among many reservations detailed in the literature, the general lack of adoption of these

Supplemental information related to this paper is available at the Journals Online website: https://doi.org/10.1175/WAF-D-21-0004.s1.

Bhardwaj's additional affiliation: India Meteorological Department, Ministry of Earth Sciences, New Delhi, India.

Corresponding author: Amit Bhardwaj, abhardwaj@fsu.edu

DOI: 10.1175/WAF-D-21-0004.1

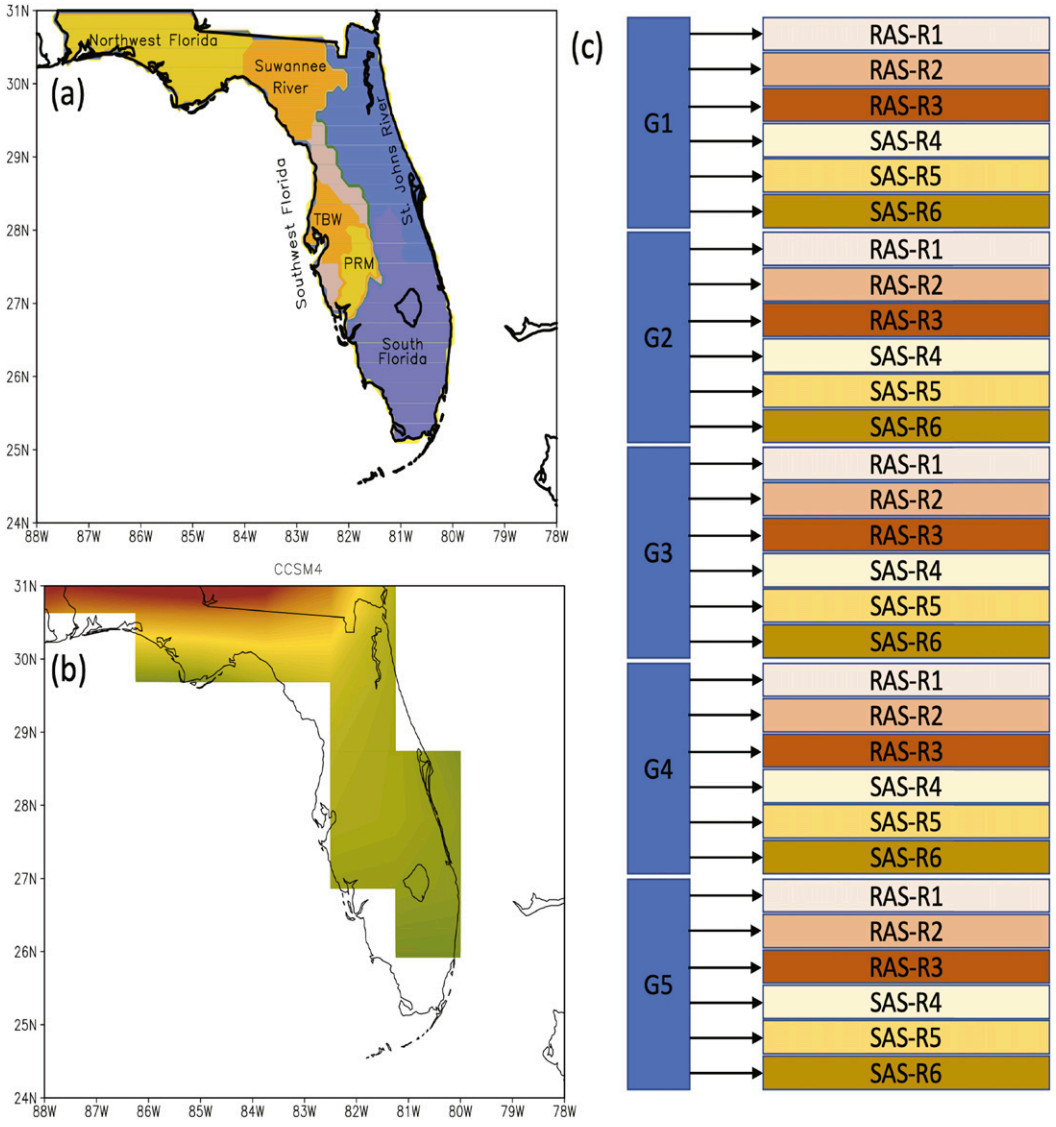

FIG. 1. (a) The subdomains outlining the five water management districts and the two water utilities (TBW and PRM) in the Southwest Florida water management district. (b) The land topography depicting the land–sea mask of CCSM4. (c) A schematic of the setup of the high-resolution experimental seasonal climate reforecasts for Florida (CLIFF). G1–G5 are the five global model seasonal reforecasts with a 1 Nov start that differ in model physics (convection scheme) and perturbations to the initial conditions of the atmosphere. R1–R6 are the RSM reforecasts conducted for each global seasonal reforecast, which differ in the width of the sponge zone (number of grid points in the sponge zone indicated) and the convection scheme [simplified Arakawa–Schubert (SAS); relaxed Arakawa–Schubert (RAS)].

seasonal forecasts is partly due to the institutional inertia, lack of awareness of such data, and risk aversion from adopting new or innovative technologies. Additionally, scale mismatch between the spatial scales of the climate forecast and the spatial scales at which the water managers require the forecasts is also a discouraging factor. This is illustrated by comparing Fig. 1a, which is at a spatial resolution of 10-km grid (a resolution that appealed to FloridaWCA stakeholders), with Fig. 1b, which is at a spatial resolution of approximately 100 km, typical of current global climate models (Kirtman et al. 2014). In Fig. 1b, the coastlines of Florida are poorly resolved, which then affects the representation of the water management districts in the global climate model.

In this study, we have downscaled seasonal climate forecasts for boreal winter at 10-km grid spacing centered over Florida. The winter season was specifically chosen for these forecasts as water managers in Florida must make relatively high-stake decisions in the following spring season. This is because the water managers plan for water allocation in the following spring season based on the prior water demand in the winter

TABLE 1. Physical parameterization schemes of the AGCM and RSM.

Physical parameterization	AGCM	RSM
Shallow convection	Tiedtke (1983)	Tiedtke (1983)
Deep convection	Three different schemes were used to generate ensemble members: 1) relaxed Arakawa–Schubert scheme (Moorthi and Suarez 1992); 2) simplified Arakawa–Schubert scheme (Hong and Pan 1998); 3) Zhang–McFarlane scheme (Zhang and McFarlane 1995)	Two different schemes were used to generate ensemble members: 1) relaxed Arakawa–Schubert scheme (Moorthi and Suarez 1992); 2) simplified Arakawa–Schubert scheme (Hong and Pan 1998)
Cloud scheme	Diagnostic cloud scheme: Slingo (1987)	Prognostic cloud scheme: Zhao and Carr (1997)
Boundary layer scheme	Hong and Pan (1996)	Hong and Pan (1996)
Gravity wave drag scheme	Alpert et al. (1988)	Alpert et al. (1988)
Shortwave radiation	Chou and Suarez (1994)	Chou and Suarez (1994)
Longwave radiation	Chou and Lee (1996)	Chou and Lee (1996)
Land surface model	Ek et al. (2003)	Ek et al. (2003)

season. The spring season is the driest season in Florida. Therefore, water allocation for spring, planned in the preceding winter season is critical to meet the anticipated demand. In unanticipated, anomalously dry winters, the water managers in some areas of Florida that critically depend on surface water have had to take costly remediation measures to mitigate the acute shortage of water in the spring. In this study, a relatively large ensemble of seasonal forecasts is made for each boreal winter season from the year 2000 to 2019, which we call seasonal reforecasts or hindcasts to assess the fidelity of the forecast system. Our eventual goal is to pursue the CLIFF hindcasts to seasonal prediction in real-time. The ensemble system developed for this project involves sampling uncertainty of the model and in initial and lateral boundary conditions. The ensemble system is necessitated by the well-established fact that climate forecasts are probabilistic, and there is economic value for end-users of the probabilistic estimates relative to a single deterministic forecast (Richardson 2006). In the following section, we provide a description of the seasonal reforecast system followed by the description of the model in section 3. Results are discussed in section 4, and conclusions are provided in section 5.

2. Model description

The atmospheric general circulation model (AGCM) used in this study follows from Kanamitsu et al. (2002b) and Misra et al. (2013). The AGCM was run at a spectral truncation of T62 (~210-km grid spacing) with model physics outlined in Table 1. The regional atmosphere model is the Regional Spectral Model (RSM) following Juang and Kanamitsu (1994), with the more recent updates to the model described in Misra et al. (2019). Like the AGCM, the RSM has 28 terrain-following vertical ($\sigma = p/p_s$) levels. The dynamical core of the RSM is based on the spectral method using sine and cosine series to solve the primitive equations (Juang and Kanamitsu 1994). It also uses a spectral damping scheme to reduce climate drift, which also allows for more substantial than conventional nesting ratios (Kanamaru and Kanamitsu 2007). The outline of the RSM physics used in this study is provided in Table 1. It may be noted that owing to the scale-selective bias correction technique in the RSM (Kanamaru and Kanamitsu 2007), the downscaling ratio far exceeds most other regional climate models and is routinely run at 10-km grid spacing from T62 spectrally truncated global models (Stefanova et al. 2012; DiNapoli and Misra 2012; Misra et al. 2018).

3. Experiment design

The high-resolution experimental seasonal climate reforecasts for Florida (CLIFF) platform is set up for real-time applications to meet the end-user requirements of our stakeholders in FloridaWCA that include the two water utilities in Central Florida (TBW and PRM) and water resource managers in the five water management districts of Florida, viz., South Florida (SF), Southwest Florida (SWF), St. Johns River (SJR), Suwannee River (SuR), and Northwest Florida (NWF; Fig. 1a). To target the relatively small watersheds of the two water utilities and the five water management districts, the horizontal resolution of CLIFF was set at 10-km grid spacing for the RSM. This particular grid spacing comes from the experience of a rich history of model simulations conducted by the authors over this region using RSM (Stefanova et al. 2012; Misra et al. 2012; Bhardwaj and Misra 2019). Higher resolutions of the RSM run at 5-km grid spacing did not yield significant benefit to the fidelity of the simulation compared to that at 10 km while it nearly consumed 6 times more computing resources for a similar domain.

The forecast set up is outlined in Fig. 1c. The AGCM and RSM are set to start on 1 November for a period of four months, until the end of February of the following year. The reforecasts or hindcasts of CLIFF were conducted over a 20-yr period from 2000 to 2019. The AGCM is forced with the SST forecast produced from another coupled GCM. This is necessary to supply lateral boundary conditions for all prognostic variables of the full atmosphere based on the global field to RSM at a 6-h interval. The SST forecast was made available at a daily interval from one of the ensemble members of the Community Climate System Model, version 4 (CCSM4), which was also initialized on 1 November. CCSM4 is part of the North American Multimodel Ensemble (NMME) suite (Kirtman et al. 2014). As the CLIFF was being set up for

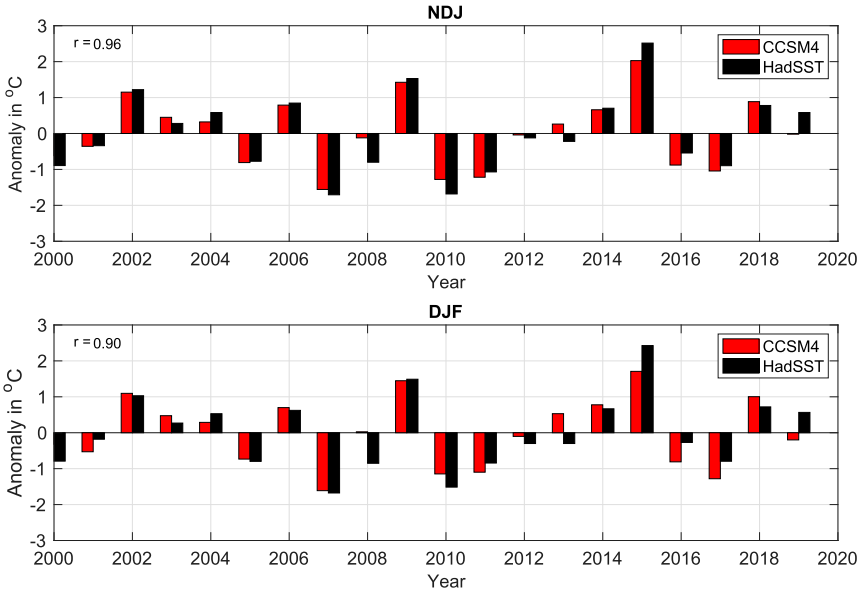

FIG. 2. The forecasted seasonal mean Niño-3.4 SST anomalies from one ensemble member of CCSM4 [as part of the North American Multimodel Ensemble project; Kirtman et al. (2014)] for (a) zero-month lead (NDJ) and (b) one-month lead (DJF) seasons with corresponding observed SST anomalies (HadSST; Rayner et al. 2003).

real-time operational forecasts, we had to rely on SST that would be available in a time-sensitive manner, which in the current arrangement with the University of Miami seemed most practical. Each of the reforecasts, were run for a period of four months, ending on 1 March. In Fig. 2, we show the seasonal forecast anomalies of SST over the Niño-3.4 region used in CLIFF at zero-month lead [November–December–January (NDJ)] and at one-month lead [December–January–February (DJF)]. These forecasted Niño-3.4 SST anomalies show an exceptionally high fidelity that bode well for CLIFF, especially regarding remote ENSO forcing.

For each season, the AGCM was run with five ensemble members (G1, ... , G5; Fig. 1b). In three of these ensemble members (G1, G2, and G5), the initial conditions of the atmosphere were perturbed. The initial conditions were obtained from the National Centers for Environmental Prediction–Department of Energy (NCEP–DOE) reanalysis (Kanamitsu et al. 2002a) of 21 October, 26 October, and 1 November, which were all reset to 1 November. In the remaining two ensemble members (G3 and G4), the atmospheric convective parameterization was changed while the initial condition was obtained from NCEP–DOE reanalysis for 1 November (Fig. 1b). For each AGCM run, six ensemble members of the RSM were run to give a total of 30 ensemble members of CLIFF for each season.

The overarching rationale for the ensembles is to optimally sample the uncertainties of the reforecasts. The uncertainties arise from initial and boundary conditions and from the model itself. In this study, we sample the uncertainties from all three sources, while also balancing the choice of the number of ensemble members per season in CLIFF with the limited computational resources available to us and practical considerations to operationalize CLIFF in the future. Of the six ensemble members of the RSM, three differed in their lateral boundary conditions, and the remaining three differed in their cumulus parameterization scheme, while all ensemble members had initial conditions of the atmosphere that differed slightly from each other.

Several studies have shown that the RSM is sensitive to lateral boundary conditions (Davies 1976; Warner et al. 1997; Marbaix et al. 2003; Misra 2006) and in RSM, the width of the relaxation zone around the lateral boundaries was found to have significant impact on the regional simulation (Kanamaru and Kanamitsu 2007).The relaxation zone around the lateral boundaries of the RSM was altered from the default 8 grid cells (R2) to 4 (R1) and 16 (R3) grid cells in three of the ensemble members (Fig. 1b). In the case when the relaxation zone was extended to 16 grid cells, the domain was slightly expanded. However, our reforecast analysis across all ensemble members uses only the interior grid cells common across all ensemble members and avoids the relaxation zone grid cells.

Many studies have noted that a significant fraction of winter rainfall in Florida is convective (Yang and Smith 2008; Tuttle and Salvucci 2016). In fact, even CLIFF displays over 40% of winter rainfall over Florida is convective (not shown). Therefore, in the remaining three ensemble members of the RSM (R4, R5, and R6; Fig. 1b), the cumulus parameterization scheme was changed in each of them from that used in R1, R2, and R3. The initial conditions of the atmosphere and land surface in RSM was obtained from NCEP–DOE reanalysis and interpolated to the RSM grid. A future version of these reforecasts will be examining the impact of land surface initialization on the seasonal prediction skill.

The verification of the reforecast skill is limited to surface precipitation and land surface temperature. Tapiador et al. (2019)

give valid arguments for precipitation being a good metric for gauging model performance. Both precipitation and surface temperature provide an integrated perspective of the 4D atmospheric state in some sense while also holding the most practical value for the stakeholders. Precipitation is verified against the daily rainfall data from the Integrated Multisatellite Retrievals for GPM, version 6 (IMERG; Huffman et al. 2019). These rainfall data are available globally at 0.1° grid spacing from 1 June 2000 to the present. Similarly, the land surface temperature is verified against the NOAA's Climate Prediction Center global daily temperature available at 0.5° grid spacing from 1979 to the present (https://psl.noaa.gov/data/gridded/data.cpc.globaltemp.html). The verification is conducted for two overlapping seasons: NDJ at zero-month lead and DJF at the one-month lead. The verification will follow both the deterministic skill measures using the ensemble mean and probabilistic skill measures that seek the advantage of the ensemble spread available from CLIFF.

4. Results

a. Deterministic skill

1) PRECIPITATION

The observed climatological rainfall from the observations for the two overlapping seasons for NDJ and DJF are shown in Figs. 3a and 3b. In both these panels, the meridional gradient of rainfall is apparent from the drier South Florida to the wetter panhandle region of Florida. The zonal gradient of rainfall is a bit more complex. There is a minimum rainfall over Peninsular Florida and higher rainfall over the Atlantic and the Gulf of Mexico, with the Atlantic receiving more than the Gulf of Mexico, north of ~30°N (Figs. 3a,b). The corresponding seasonal climatology from CLIFF is shown in Figs. 3c and 3d. These figures clearly show that CLIFF is overestimating the seasonal rainfall climatology. However, CLIFF seems to verify the observed meridional gradient of the rainfall reasonably. The observed zonal gradient of precipitation is preserved in CLIFF across the South Florida region but is compromised in North Florida, especially in the DJF season with excessive rainfall over the Florida Panhandle (Fig. 3d). The systematic seasonal mean errors from CLIFF for NDJ (Fig. 3e) and DJF (Fig. 3f) substantiate the overestimation, which is both over land and ocean. The overestimation is slightly more exacerbated in DJF than in NDJ season. Some of these systematic errors displayed by the RSM could be influenced by the bias in the parent AGCM while others could be related to errors within RSM.

The area-averaged rainfall over the seven subdomains outlined in Fig. 1a is shown for each of the seasons from observations and CLIFF in Figs. 4a–n. The overestimation of the rainfall over all subdomains in both overlapping seasons is evident in Fig. 4. The magnitude of the observed seasonal mean rain is on the lower fringe or outside of the ensemble range of CLIFF for some subdomains (Figs. 4a–l). None of the choices of the cumulus parameterization schemes or choices of the width of the relaxation zone in RSM appeared to have systematically higher simulation skill than others across all years (not shown).

The interannual variations of the NDJ mean rainfall in CLIFF is reasonably well depicted, especially over SJR (Fig. 4c), SWF (Fig. 4d), SF (Fig. 4e), and in the watersheds of PRM (Fig. 4f) and TBW (Fig. 4g)The anomaly correlations between the ensemble mean and the corresponding observations are 0.64, 0.71, 0.7, 0.77, and 0.67, respectively. Over NWF (Fig. 4a) and SuR (Fig. 4b), the reforecast skills of seasonal precipitation in NDJ are comparatively smaller with anomaly correlations at 0.44 and 0.34, respectively. In the following overlapping season of the DJF, the anomaly correlations of the seasonal precipitation anomalies in CLIFF uniformly decrease across all subdomains relative to NDJ (Figs. 4h–n). This deterioration in skill at one-month lead could be argued as a result of the model drift dominating over the memory of the initial condition of the climate system. It may be noted that in both NDJ and DJF seasons, the trend of seasonal rainfall is insignificant, as noted by the comparable correlations with inclusion and exclusions of the trend in Fig. 4.

2) SURFACE TEMPERATURE

The observed seasonal mean climatology for NDJ and DJF seasons are shown in Figs. 5a and 5b, respectively. The relatively coarse resolution of the observed dataset at 0.5° grid spacing makes the coastlines slightly jagged (Figs. 5a,b). Nonetheless, the observed large-scale meridional gradient of temperature from north to south is quite apparent, with the zonal variations in temperature being far smaller. The corresponding seasonal climatology from CLIFF is shown in Figs. 5c and 5d. It may be recalled that ocean temperatures are prescribed and are obtained from the seasonal reforecast made with CCSM4. The winter hydroclimate over Florida is found to be less sensitive to the SST anomalies in the neighboring oceans compared to that over remote oceans (Nag et al. 2014; Misra and Bhardwaj 2020). The land surface temperature in CLIFF picks the observed large-scale meridional gradient reasonably well (Figs. 5c,d) while keeping the zonal gradient small like the observations. The systematic errors of CLIFF (Figs. 5e,f) show that the errors remain relatively comparable between NDJ and DJF seasons, unlike the precipitation errors. It is apparent from Figs. 5e and 5f that CLIFF displays a systematic cold bias.

The area-averaged surface temperature over the seven subdomains in Figs. 6a–g for NDJ and Figs. 6h–n for DJF show more sobering results for CLIFF compared to seasonal precipitation skill in Fig. 4. The surface temperature trend both in the observations and CLIFF are comparable and is apparent across all subdomains (Fig. 6). The observed surface temperature also falls within the ensemble range of CLIFF in many instances across subdomains and seasons (Fig. 6), unlike those for precipitation in Fig. 4. However, the correlations of the seasonal surface temperature anomalies show that the ensemble means of CLIFF exhibit relatively weaker skill (Fig. 6) than precipitation (Fig. 4). For example, the highest anomaly correlation in the NDJ season is over SF and at 0.17 (Fig. 6e). Interestingly, the anomaly correlations of the seasonal surface temperature in the DJF season improve and range from 0.17 over SF (Fig. 6l) to 0.39 over SuR (Fig. 6i). This could be the impact of variations in the land–atmosphere coupling. The land–atmosphere coupling in general refers to the interactions

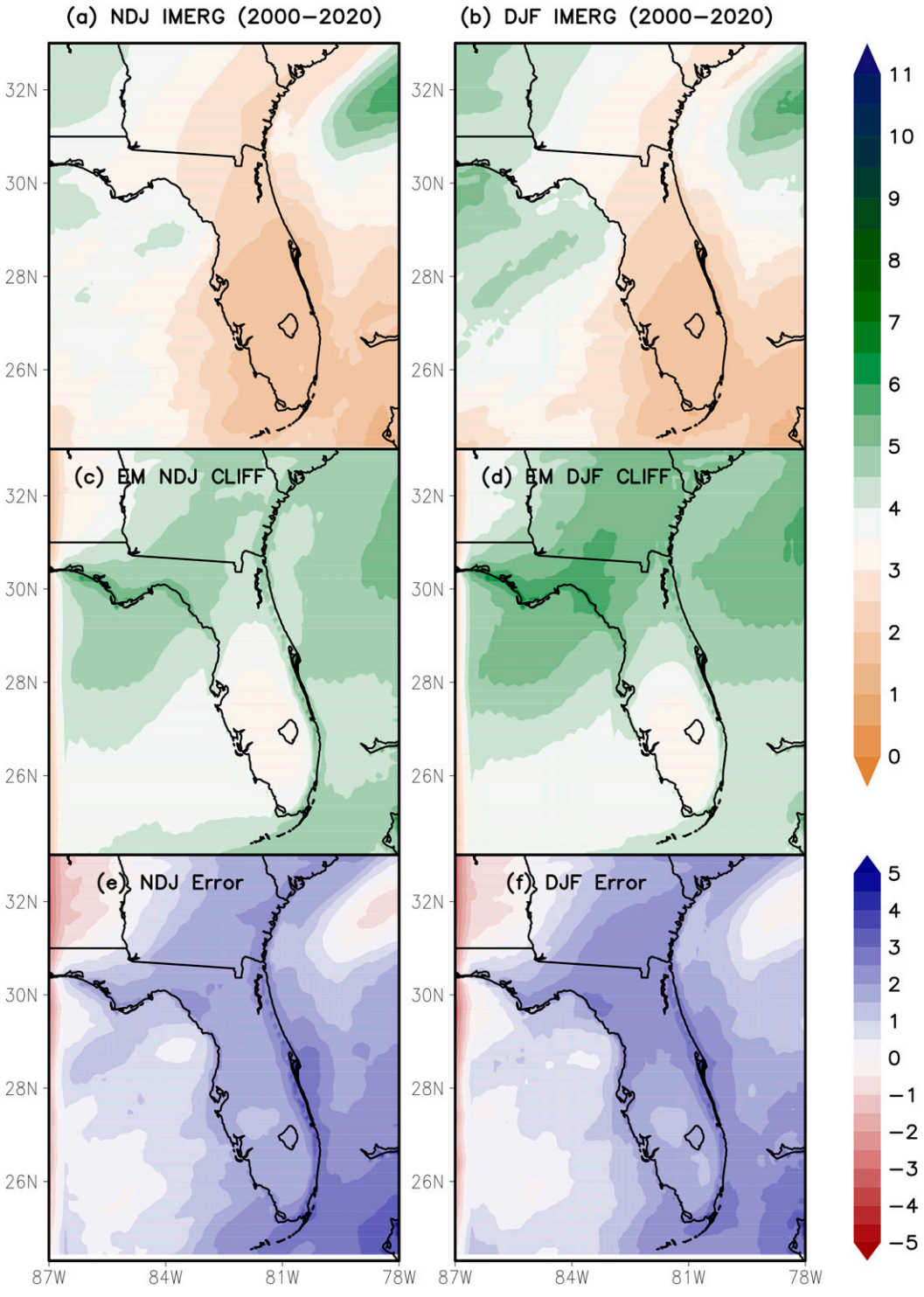

FIG. 3. Climatological seasonal mean precipitation (mm day^{-1}) for (a),(c) November–December–January (NDJ) and (b),(d) December–January–February (DJF) from (top) IMERG and (middle) ensemble mean CLIFF. Note that NDJ and DJF are at zero-month and one-month forecast lead, and DJF is a one-month forecast lead, respectively, in CLIFF. The corresponding climatological errors (CLIFF-IMERG; mm day^{-1}) are shown for (e) NDJ and (f) DJF seasons.

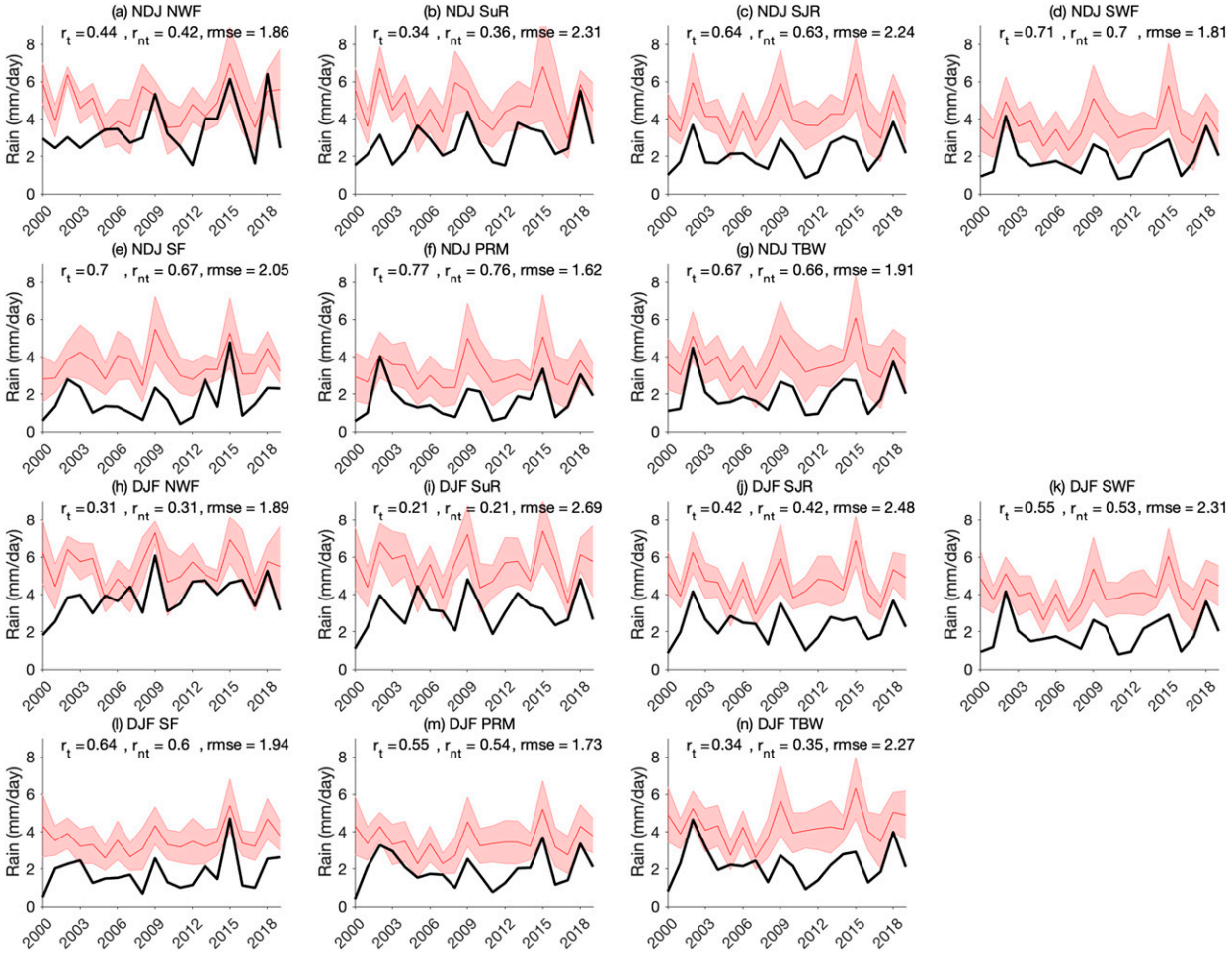

FIG. 4. Time series of (top) NDJ and (bottom) DJF seasonal mean precipitation (mm day^{-1}) from IMERG (black line) and for CLIFF (red line is for the ensemble mean, and shading is the range of the ensemble members) for (a),(h) Northwest Florida (NWF); (b),(i) Suwannee River; (c),(j) St. Johns River; (d),(k) Southwest Florida (SWF); (e),(l) South Florida (SF); (f),(m) Peace River Manasota (PRM); and (g),(n) Tampa Bay Water regions. The correlation between the IMERG observations and ensemble mean CLIFF with the trend (r_t) and after removing trend (r_{nt}) and the corresponding root-mean-square error (rmse) are also indicated.

between soil moisture and precipitation (Misra 2020). To ascertain this, we compute in Table 2 the seasonality of this land–atmosphere coupling strength using the terrestrial coupling index (TCI) following Dirmeyer (2011) and the atmosphere coupling index (ACI) following Dirmeyer et al. (2014). They are given by

$$\mathrm{TCI} = \sigma_F r(F, L), \tag{1}$$

$$\mathrm{ACI} = \sigma_A r(A, F), \tag{2}$$

where F refers to latent and sensible heat flux, and L refers to the land state variable, which in our case is the root zone soil wetness, and A refers to the atmospheric state, which we choose to be 2-m air (or surface) temperature. Dirmeyer (2011) suggest that TCI measures the land segment of the land–atmosphere coupling strength by examining the relation between soil moisture and surface fluxes. The atmospheric segment of the land–atmosphere coupling is accounted for in ACI, which measures the impact of the surface fluxes on the air temperature (Dirmeyer et al. 2014). In Table 2, we observe that the TCI increases from November to February while the ACI is insignificant and does not show a subseasonal evolution. The increase in TCI is consistent with the seasonal evolution of the hydroclimate over Florida when it gets drier from winter to spring. It is apparent from Table 2 that the land segment of the land–atmosphere coupling pathway has a stronger monthly variation. This coupling is via the thermally driven pathway of the energy cycle, with the role of the sensible heat flux dominating over the latent heat flux in modulating the root zone soil wetness. Therefore, the increase in the correlations of CLIFF observed in Fig. 6 is consistent with the monthly evolution of the land–atmosphere coupling strength. However, the atmospheric segment of the land–atmosphere coupling is much weaker (Table 2), which explains the relatively weak correlations of CLIFF surface temperature with corresponding observations (Fig. 6).

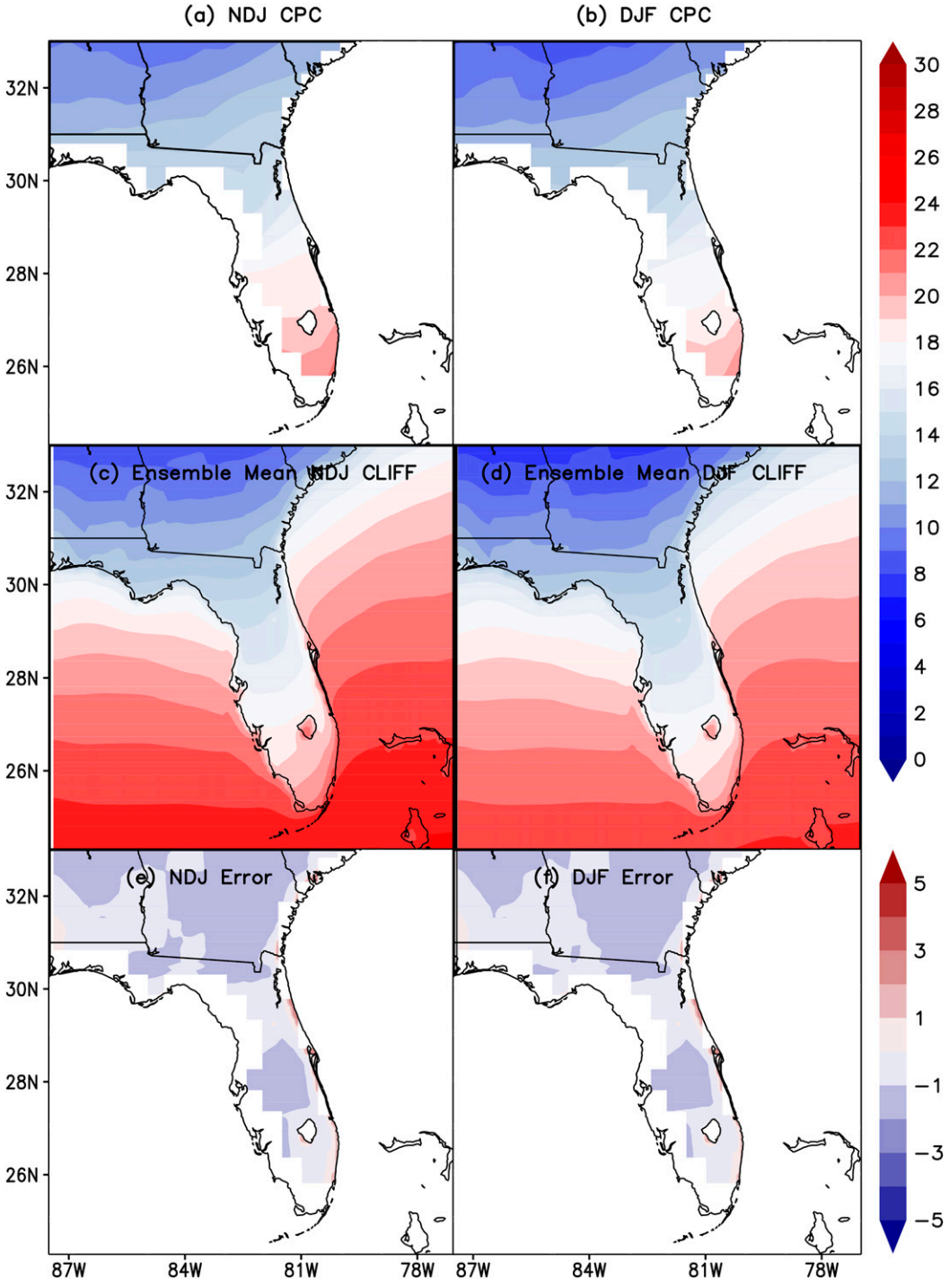

FIG. 5. Climatological seasonal mean surface temperature (°C) for (a),(c) NDJ and (b),(d) DJF from (top) CPC and (middle) ensemble mean CLIFF. Note that NDJ and DJF are a zero-month and one-month forecast lead, respectively, in CLIFF. The corresponding climatological errors (CLIFF-CPC; °C) are shown for (e) NDJ and (f) DJF seasons.

It is interesting to note that these correlations in surface temperature drop precipitously when the linear trend is removed both from observations and CLIFF, suggesting that most of the seasonal prediction skill in land surface temperature in CLIFF is coming from the long-term warming trend (Fig. 6).

b. *Probabilistic skill*

Although quantifying the deterministic skill is convenient and provides a quick look at the fidelity of the seasonal reforecasts, it is far from a complete picture. Branković and Palmer (1997)

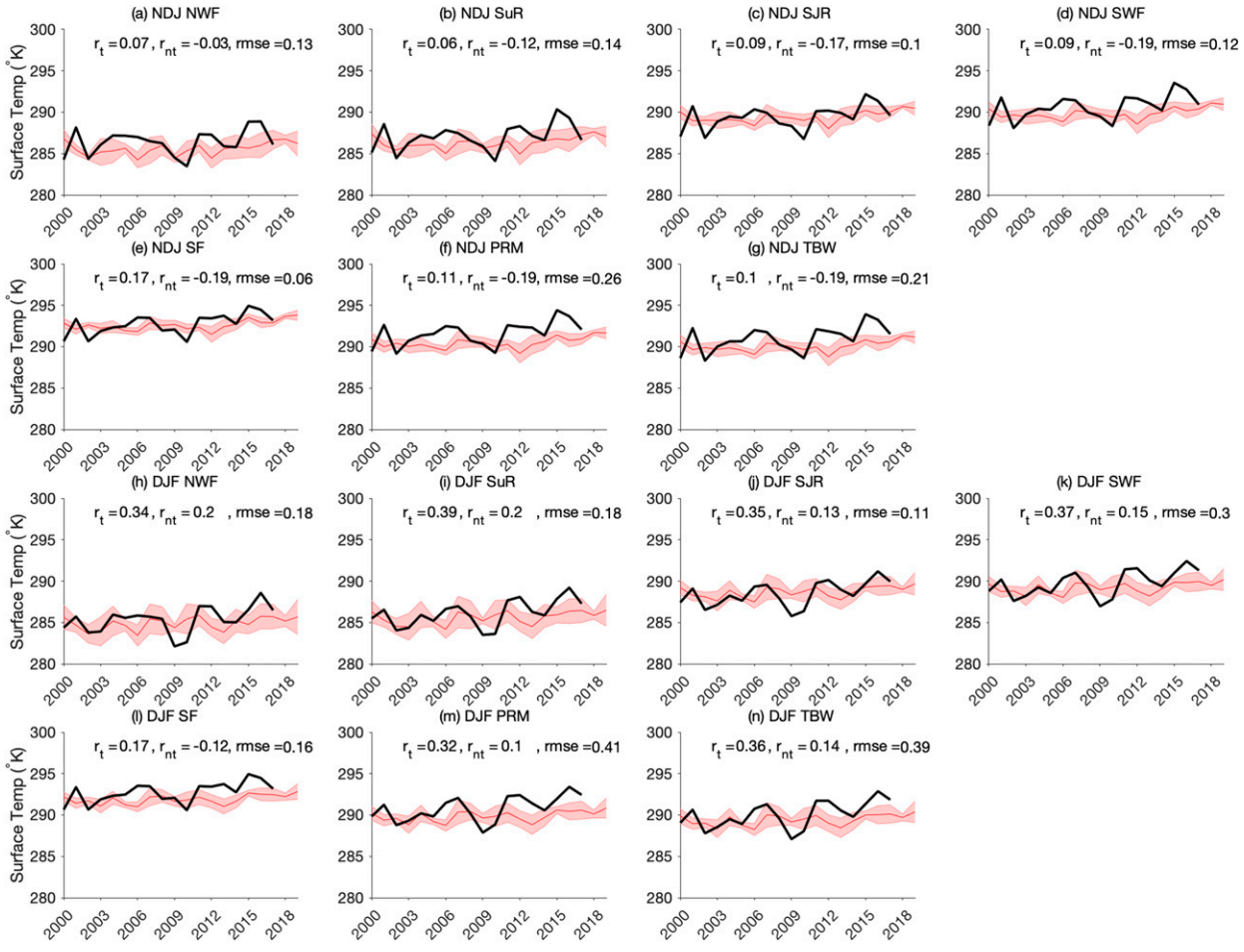

FIG. 6. Time series of (top) NDJ and (bottom) DJF seasonal mean land surface temperature (°C) from CPC (black line) and for CLIFF (red line is for the ensemble mean and shading is the range of the ensemble members) for (a),(h) Northwest Florida (NWF); (b),(i) Suwannee River; (c),(j) St. Johns River; (d),(k) Southwest Florida (SWF); (e),(l) South Florida (SF); (f),(m) Peace River Manasota (PRM); and (g),(n) Tampa Bay Water regions. The correlation between the CPC observations and ensemble mean CLIFF with the trend (r_t) and after removing trend (r_{nt}) and the corresponding root-mean-square error (rmse) are also indicated.

indicate that the slowly varying lower boundary conditions (e.g., SST, soil moisture) assert their impact on the phase-space geometry of the whole atmospheric climate attractor rather than on a single phase-space trajectory. Therefore, the study suggests that the changes to the atmospheric probability distribution function over different atmospheric states have to be assessed to estimate the seasonal climate prediction skill of reforecasts like CLIFF. Many other

TABLE 2. Seasonality of the land–atmosphere coupling strength in CLIFF (bold values indicate that it is significant at a 5% significance level). LHF = latent heat flux; RSW = root zone soil wetness; SHF = sensible heat flux; T2M = 2-m air temperature.

Subdomain	Terrestrial coupling index (TCI)								Atmospheric coupling index (ACI)							
	$\sigma_{LHF}r$(LHF, RSW)				$\sigma_{SHF}r$(SHF, RSW)				$\sigma_{T2M}r$(LHF, T2M)				$\sigma_{T2M}r$(SHF, T2M)			
	Nov	Dec	Jan	Feb	Nov	Dec	Jan	Feb	Nov	Dec	Jan	Feb	Nov	Dec	Jan	Feb
NWF	0.4	0.3	−0.1	**0.6**	**−0.6**	−0.2	−0.2	**−0.9**	−0.1	0.1	0.1	−0.1	0.1	−0.2	−0.1	0.1
SuR	0.3	0.2	−0.1	0.3	**−0.6**	−0.04	−0.2	**−0.8**	−0.1	−0.1	0.01	−0.1	−0.01	−0.1	0.1	0.13
SJR	0.3	**0.9**	0.3	**0.6**	**−0.7**	−0.2	−0.3	**−0.9**	−0.1	−0.2	−0.2	−0.2	−0.3	−0.04	−0.04	0.05
SWF	0.3	**0.5**	**0.7**	**0.8**	**−0.5**	−0.4	**−0.5**	**−0.8**	−0.2	−0.2	−0.2	−0.2	−0.2	0.03	0.01	0.1
SF	0.3	**0.6**	**0.5**	0.4	**−1.1**	**−0.5**	**−0.7**	**−0.6**	0.1	−0.1	−0.1	−0.1	−0.2	0	0.02	−0.1
PRM	−0.04	0.3	0.3	**0.6**	**−0.6**	−0.4	**−0.6**	**−0.7**	−0.1	−0.1	−0.1	−0.1	−0.2	0.1	0.1	0.01
TBW	**0.8**	**0.9**	**1.2**	**1.4**	−0.3	−0.4	**−0.5**	**−0.8**	−0.2	−0.2	−0.2	−0.2	−0.2	−0.04	−0.05	0.03

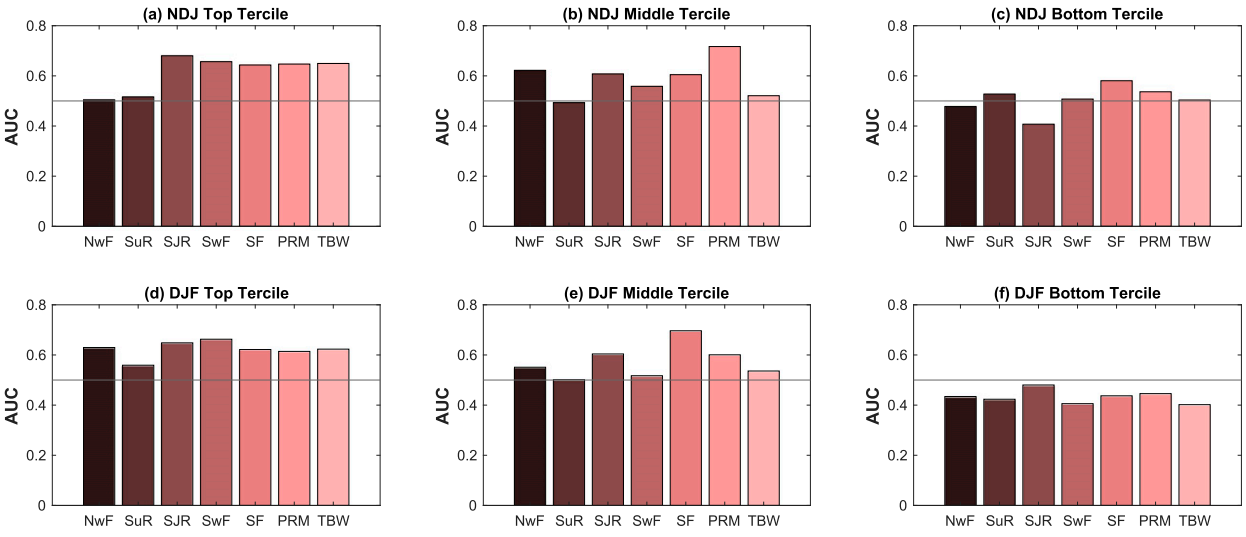

FIG. 7. The area under the relative operating characteristic curves (AUC) for (top) zero-month lead NDJ and (bottom) one-month DJF seasonal rainfall anomaly in the (a),(d) top; (b),(e) middle; and (c),(f) bottom tercile over Northwest Florida (NWF), Suwannee River (SuR), St. Johns River (SJR), Southwest Florida (SWF), South Florida (SF), Peace River Manasota (PRM), and Tampa Bay Water (TBW) subdomains. The black horizontal line at 0.5 represents the AUC score for climatology.

studies spanning over several decades have also strongly advocated using probability skill measures (Palmer et al. 2000; Richardson 2000; Palmer 2002; Kirtman et al. 2014). In this study, we analyze the probabilistic skill measure of CLIFF using the area under the relative operating characteristic curves (AUC) under different probability thresholds (detailed further in the online supplemental material). The probability thresholds that we examine are terciles [below normal (bottom tercile), above normal (top tercile), and normal (middle tercile)] and pentiles [P1(bottom pentile), P2, P3, P4, P5(top pentile)] on seasonal surface temperature and precipitation anomalies for the seven subdomains. The threshold limits for terciles and pentiles for seasonal temperature and precipitation from both observations and CLIFF for all seven subdomains are provided in a tabular format in the supplemental material.

1) PRECIPITATION

Figures 7a–f show the AUC for the NDJ and the DJF seasonal precipitation anomalies over the seven subdomains where terciles define the thresholds. When AUC is at or below the value of 0.5, it indicates that the forecast has no skill, or the forecast skill is no better than climatology or a random forecast (Graham et al. 2000). In Fig. 7, we find that usually, the AUC of CLIFF is above 0.5. However, when the DJF precipitation anomalies reside in the bottom tercile (drought anomalies) then CLIFF displays values of AUC of around 0.4 (Fig. 7f). There are, however, other exceptions when CLIFF displays AUC $\leq$ 0.5, like over NWF (Fig. 7a), SuR (Fig. 7b), NWF, and SJR (Fig. 7c). CLIFF displays the highest skill for the anomalous wet (top tercile) events in both NDJ and DJF seasons (Fig. 7). Similarly, CLIFF displays the least skill for the drought (bottom tercile) events of seasonal precipitation (Fig. 7). This is not surprising as anomalous wet winters in Florida are usually related to warm ENSO variations, which are typically larger in magnitude relative to the cold ENSO events (Kumar and Hoerling 1998). Hoerling et al. (1997) suggested that the nonlinearity of the stationary wave response to ENSO anomalies between El Niño and La Niña is significant over the North American region. Their study revealed that the circulation anomalies over North America are slightly larger for the warm versus cold tropical SST states, suggesting that El Niño teleconnections could be stronger. Furthermore, as observed in Fig. 3, the RSM has a wet mean bias in the winter that likely further affects its ability to simulate drier winter seasonal anomalies over Florida. More recently, Nag et al. (2014) indicate decadal modulation of ENSO-forced winter anomalies in the Southeastern U.S. including over Florida. However, this variability cannot be investigated from CLIFF hindcasts on account of the relatively short span of years covered in the dataset.

We extend this analysis further by computing AUC for thresholds based on pentiles (Figs. 8a–f). The stakeholders in FloridaWCA have a very keen interest in extreme rain anomalies. Given the spatial resolution, limited ensemble members per season, and the number of years of hindcasts of CLIFF, pentiles were considered a good compromise to address extreme anomalies. In contrast to the tercile rain events (Fig. 7), the pentile rain events in Fig. 8 show that there are far more instances of CLIFF displaying AUC $\leq$ 0.5. The slight deterioration in the probabilistic seasonal precipitation skill of CLIFF from tercile to pentile events is a reflection of a combination of several factors. They include that pentile events reduce sample size relative to terciles, there is inadequate ensemble size of CLIFF to predict pentile events, and model bias becomes more significant for pentile than tercile events. Nonetheless, CLIFF consistently shows useful probabilistic skill (AUC $\geq$ 0.5) for a large fraction of the subdomains and

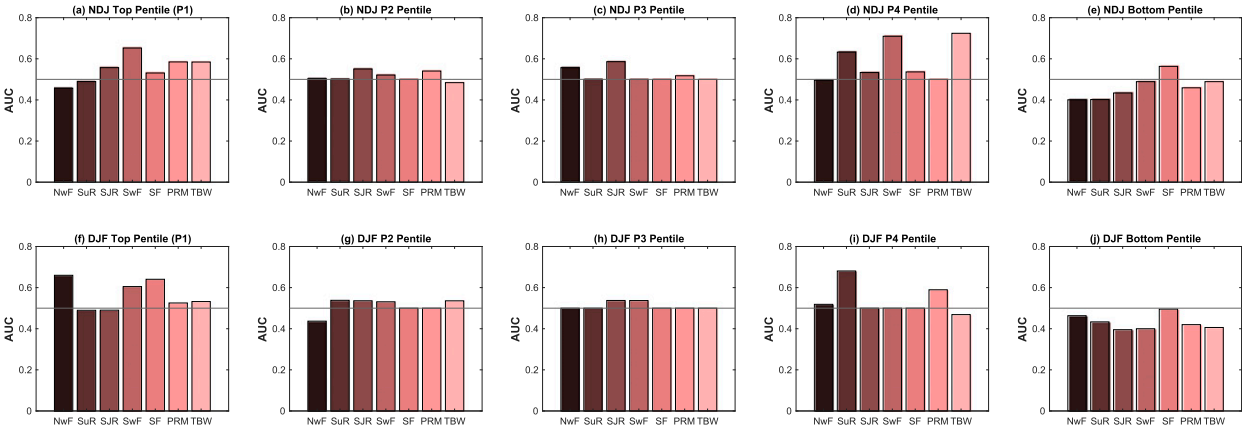

FIG. 8. The area under the relative operating characteristic curves (AUC) for (top) zero-month lead NDJ and (bottom) one-month DJF seasonal rainfall anomaly in the (a),(f) top; (b),(g) second; (c),(h) third; (d),(i) fourth; and (e),(j) bottom pentile over Northwest Florida (NWF), Suwannee River (SuR), St. Johns River (SJR), Southwest Florida (SWF), South Florida (SF), Peace River Manasota (PRM), and Tampa Bay Water (TBW) subdomains. The black horizontal line at 0.5 represents the AUC score for climatology.

pentile seasonal precipitation thresholds. We also find that seasonal precipitation events associated with the top pentile (P1 or wet) events display higher skill in CLIFF than events associated with the bottom pentile (P5 or drought) events.

2) SURFACE TEMPERATURE

The AUC for the tercile thresholds of land surface temperature is shown in Fig. 9. Unlike the deterministic skill shown in Fig. 6, the probabilistic measure of AUC in Fig. 9 shows that CLIFF displays useful skill across most subdomains with AUC ≥ 0.5. Skill is evident especially for events in the top (warm events) and middle (neutral events) tercile. This again highlights the usefulness of the ensemble strategy over a deterministic approach. The AUC of CLIFF for the pentile events of seasonal surface temperature anomalies in Fig. 10 shows a slight deterioration of the skill from those for terciles in Fig. 9. Furthermore, unlike the deterministic skill (Fig. 6), the differences in the probabilistic skill between the NDJ and the DJF seasons for both terciles and pentiles are relatively insignificant.

5. Conclusions

This paper introduced climate reforecasts for Florida (CLIFF), a dynamical seasonal prediction strategy for boreal winter over Florida. CLIFF was designed to meet the demands of stakeholders in water utilities and water management districts of Florida. The stakeholders desired a Florida specific seasonal

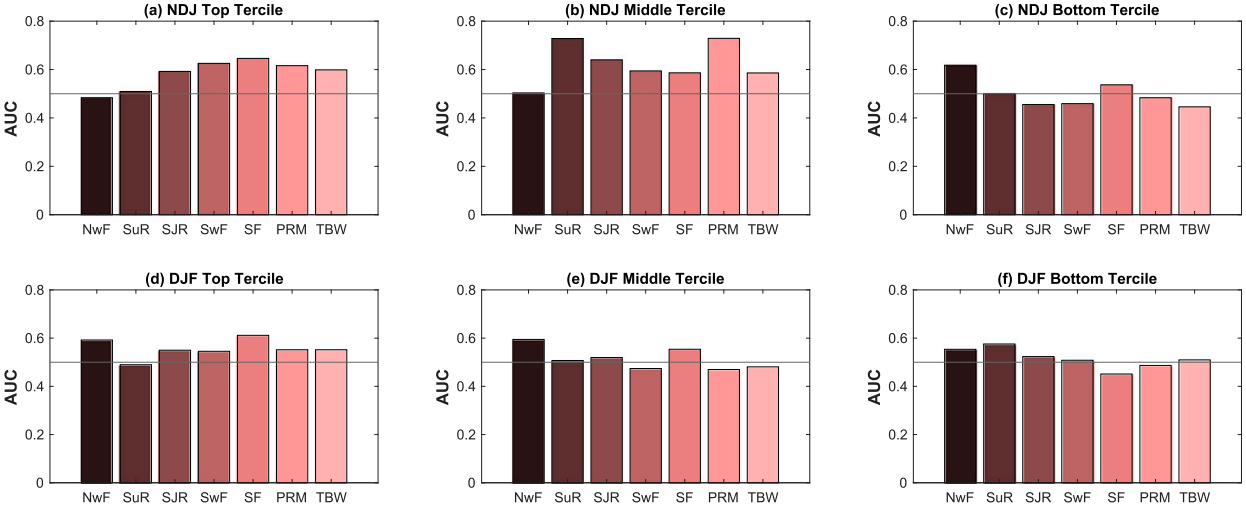

FIG. 9. The area under the relative operating characteristic curves (AUC) for (top) zero-month lead NDJ and (bottom) one-month DJF seasonal land surface temperature anomaly in the (a),(d) top; (b),(e) middle; and (c),(f) bottom tercile over Northwest Florida (NWF), Suwannee River (SuR), St. Johns River (SJR), Southwest Florida (SWF), South Florida (SF), Peace River Manasota (PRM), and Tampa Bay Water (TBW) subdomains. The black horizontal line at 0.5 represents the AUC score for climatology.

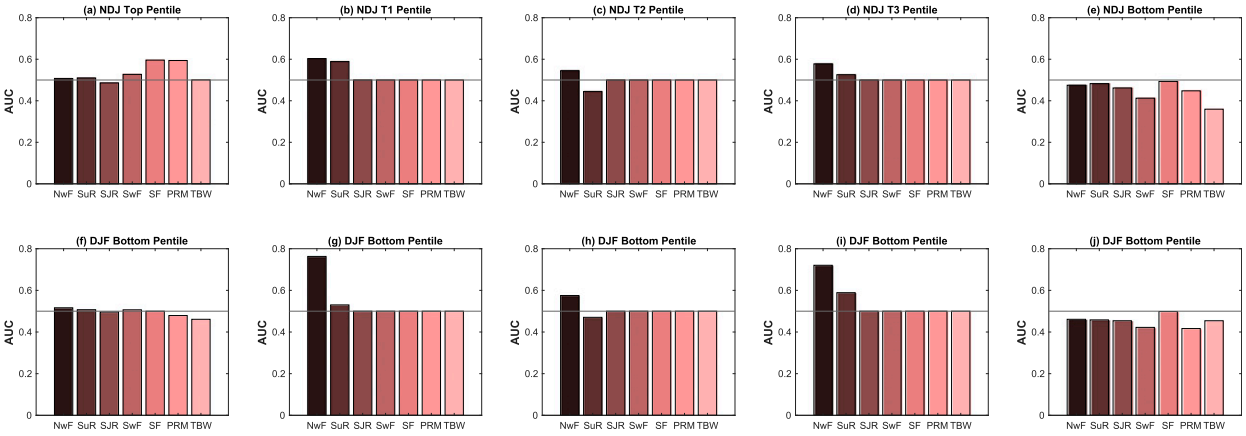

FIG. 10. The area under the relative operating characteristic curves (AUC) for (top) zero-month lead NDJ and (bottom) one-month DJF seasonal land surface temperature anomaly in the (a),(f) top; (b),(g) second; (c),(h) third; (d),(i) fourth; and (e),(j) bottom pentile over Northwest Florida (NWF), Suwannee River (SuR), St. Johns River (SJR), Southwest Florida (SWF), South Florida (SF), Peace River Manasota (PRM), and Tampa Bay Water (TBW) subdomains. The black horizontal line at 0.5 represents the AUC score for climatology.

climate prediction at the highest possible spatial resolution. CLIFF is unique in that the prediction is made at a relatively high spatial resolution of 10-km grid spacing focused on the five water management districts of Florida, which also includes the watersheds of two water utilities in Central Florida (TBW and PRM) that participated in the design of CLIFF. CLIFF uses a regional atmospheric model to downscale seasonal forecasts from an AGCM forced by SST. The SST is produced by a single ensemble member of a model in the NMME (CCSM4). CLIFF produces an ensemble of 30 members per season. The ensemble members of CLIFF are generated from perturbing the lateral boundary conditions by varying the width of the relaxation zone and varying the cumulus parameterization scheme in the regional atmospheric model.

CLIFF produces the largescale features of the climatological boreal winter season precipitation and land surface temperature reasonably well. These large-scale features are characterized by atypical zonal and meridional gradients in the region that CLIFF can simulate, although there is a systematic wet and cold bias.

The deterministic and probabilistic skill analysis of CLIFF for two overlapping seasons of NDJ (zero-month lead) and DJF (one-month lead) indicate that CLIFF produces useful forecast skill of seasonal precipitation and surface temperature anomalies. For example, the seasonal prediction skill of precipitation from CLIFF over all seven subdomains (Fig. 1a) shows anomaly correlations ranging from 0.34 to 0.76 in the NDJ season and with AUC mostly at or above 0.5. At the subsequent overlapping DJF season, the prediction skill of CLIFF deteriorates slightly. On the other hand, the deterministic skill of surface temperature from CLIFF is more sobering, with the warming trend contributing most of the useful skill. Some of this poor deterministic skill of surface temperature in CLIFF is inherent to the weak atmospheric segment of the land–atmosphere coupling. However, under probabilistic skill measures, the land surface temperature skills from CLIFF indicate that they are useful with AUC at or near 0.5.

This study also shows that developing such regional climate forecast systems highlights the benefit of high-resolution forecasts. For example, stakeholders in FloridaWCA have questioned the implementation of such forecast systems as CLIFF when it is common knowledge that a developing ENSO is likely to impact Florida in a particular way. In other words, they suggest that ENSO forecasts should be sufficient to derive a heuristic forecast for Florida winters. This heuristic forecast is, however, misleading for the granularity of the information content that the stakeholders seek, given that ENSO impact over Florida is nonuniform and has other associated low-frequency variations (Nag et al. 2014; Misra et al. 2017). This study also shows that across the five water management districts, the impact of ENSO on surface temperature and rainfall is nonuniform. Furthermore, the seasonal winter predictability displayed by CLIFF across the five water management districts is also nonuniform. No two ENSOs are alike. For example, similar amplitude ENSO events, like the El Niño events of 2006 and 2018 (Fig. 2), had a disproportionate impact on rainfall across Florida (Fig. 4). Similarly, we found that the seasonality of the land–atmosphere coupling strength affects the predictability of the land surface temperature in CLIFF. Thus, it would be ill-advised to solely bank on the heuristic skills of ENSO teleconnection over Florida.

CLIFF, however, has some limitations. Foremost is that the regional model is forced by SSTs from one GCM (CCSM4), which limits the sampling of the uncertainty in the forecast of SST. Another limitation is that CLIFF is not offering a certain, deterministic forecast that verifies with observations, which the water managers prefer for their decision support system. Although, the probabilistic measures of the forecasts produced by CLIFF is encouraging, it is not useful to the water managers at the present. Currently, the water managers are forced to make conservative decisions on water management that are potentially expensive but mitigate risk from unanticipated climate anomalies. TBW is now currently running scenarios of their watershed model based purely on CLIFF forecasts

instead of using climatology to seek its true value in their decision support system. We will report the results of their analysis with the real-time forecast skills of CLIFF in the near future.

Acknowledgments. Grants from NASA Grant NNX17AG72G supported this work. The supercomputing facility provided by the Florida State University High-Performance Computing Cluster was used to complete the model integrations analyzed in this study. CPC global temperature data are provided by the NOAA/OAR/ESRL PSL, Boulder, Colorado, from their website at https://psl.noaa.gov/, and the IMERG rainfall was obtained from https://gpm.nasa.gov/data-access/downloads/gpm.

REFERENCES

Alpert, J. C., M. Kanamitsu, P. M. Caplan, J. G. Sela, G. White, and E. Kalnay, 1988: Mountain induced gravity wave drag parameterization in the NMC medium-range forecast model. Preprints, *Eighth Conf. on Numerical Weather Prediction*, Baltimore, MD, Amer. Meteor. Soc., 726–733.

Bastola, S., and V. Misra, 2013: Sensitivity of hydrological simulations of southeastern United States watersheds to temporal aggregation of rainfall. *J. Hydrometeor.*, **14**, 1334–1344, https://doi.org/10.1175/JHM-D-12-096.1.

Bhardwaj, A., and V. Misra, 2019: The role of air-sea coupling in the downscaled hydroclimate projection over Peninsular Florida and the West Florida Shelf. *Climate Dyn.*, **53**, 2931–2947, https://doi.org/10.1007/s00382-019-04669-5.

Bolson, J., C. Martinez, N. Breuer, P. Srivastava, and P. Knox, 2013: Climate information use among southeast U.S. water managers: Beyond barriers and toward opportunities. *Reg. Environ. Change*, **13**, 141–151, https://doi.org/10.1007/s10113-013-0463-1.

Branković, C., and T. N. Palmer, 1997: Atmospheric seasonal predictability and estimates of ensemble size. *Mon. Wea. Rev.*, **125**, 859–874, https://doi.org/10.1175/1520-0493(1997)125<0859:ASPAEO>2.0.CO;2.

Chou, M.-D., and M. J. Suarez, 1994: An efficient thermal infrared radiation parameterization for use in general circulation models. National Aeronautics and Space Administration, Goddard Space Flight Center, 85 pp.

——, and K.-T. Lee, 1996: Parameterizations for the absorption of solar radiation by water vapor and ozone. *J. Atmos. Sci.*, **53**, 1203–1208, https://doi.org/10.1175/1520-0469(1996)053<1203:PFTAOS>2.0.CO;2.

Davies, H. C., 1976: A lateral boundary formulation for multi-level prediction models. *Quart. J. Roy. Meteor. Soc.*, **102**, 405–418, https://doi.org/10.1002/qj.49710243210.

DiNapoli, S., and V. Misra, 2012: Reconstructing the 20th century high-resolution climate of the southeastern United States. *J. Geophys. Res.*, **117**, D19113, https://doi.org/10.1029/2012JD018303.

Dirmeyer, P. A., 2011: The terrestrial segment of soil moisture climate coupling. *Geophys. Res. Lett.*, **38**, L16702, https://doi.org/10.1029/2011GL048268.

——, Z. Wang, M. J. Mbuh, and H. E. Norton, 2014: Intensified land surface control on boundary layer growth in a changing climate. *Geophys. Res. Lett.*, **41**, 1290–1294, https://doi.org/10.1002/2013GL058826.

Dow, K., R. E. O'Connor, B. Yarnal, G. J. Carbone, and C. L. Jocoy, 2007: Why worry? Community water system managers' perceptions of climate vulnerability. *Global Environ. Change*, **17**, 228–237, https://doi.org/10.1016/j.gloenvcha.2006.08.003.

Ek, M. B., K. E. Mitchell, Y. Lin, E. Rogers, P. Grunmann, V. Koren, G. Gayno, and J. D. Tarpley, 2003: Implementation of Noah land surface model advances in the National Centers for Environmental Prediction operational mesoscale Eta model. *J. Geophys. Res.*, **108**, 8851, https://doi.org/10.1029/2002JD003296.

Graham, R. J., A. D. L. Evans, K. R. Mylne, M. S. J. Harrison, and K. B. Robertson, 2000: An assessment of seasonal predictability using atmospheric general circulation models. *Quart. J. Roy. Meteor. Soc.*, **126**, 2211–2240, https://doi.org/10.1256/smsqj.56711.

Hoerling, M. P., A. Kumar, and M. Zhong, 1997: El Niño, La Niña, and the nonlinearity of their teleconnections. *J. Climate*, **10**, 1769–1786, https://doi.org/10.1175/1520-0442(1997)010<1769:ENOLNA>2.0.CO;2.

Hong, S.-Y., and H. L. Pan, 1996: Nonlocal boundary layer vertical diffusion in a medium-range forecast model. *Mon. Wea. Rev.*, **124**, 2322–2339, https://doi.org/10.1175/1520-0493(1996)124<2322:NBLVDI>2.0.CO;2.

——, and H.-L. Pan, 1998: Convective trigger function for a mass flux cumulus parameterization scheme. *Mon. Wea. Rev.*, **126**, 2599–2620, https://doi.org/10.1175/1520-0493(1998)126<2599:CTFFAM>2.0.CO;2.

Huffman, G. J., R. F. Adler, D. T. Bolvin, K. Hsu, C. Kidd, E. J. Nelkin, J. Tan, and P. Xie, 2019: Algorithm Theoretical Basis Document (ATBD) for Global Precipitation Climatology Project Version 3.0 Precipitation Data. NASA GSFC, 27 pp.

Juang, H. M., and M. Kanamitsu, 1994: The NMC nested regional spectral model. *Mon. Wea. Rev.*, **122**, 3–26, https://doi.org/10.1175/1520-0493(1994)122<0003:TNNRSM>2.0.CO;2.

Kanamaru, H., and M. Kanamitsu, 2007: Scale selective bias correction in a downscaling of global analysis using a regional model. *Mon. Wea. Rev.*, **135**, 334–350, https://doi.org/10.1175/MWR3294.1.

Kanamitsu, M., W. Ebisuzaki, J. Woollen, S. K. Yang, J. J. Hnilo, M. Fiorino, and G. L. Potter, 2002a: NCEP–DOE AMIP-II Reanalysis (R-2). *Bull. Amer. Meteor. Soc.*, **83**, 1631–1644, https://doi.org/10.1175/BAMS-83-11-1631.

——, and Coauthors, 2002b: NCEP dynamical seasonal forecast system 2000. *Bull. Amer. Meteor. Soc.*, **83**, 1019–1037, https://doi.org/10.1175/1520-0477(2002)083<1019:NDSFS>2.3.CO;2.

Kirtman, B. P., and Coauthors, 2014: The North American Multimodel Ensemble: Phase-1 seasonal-to-interannual prediction; Phase-2 toward developing intraseasonal prediction. *Bull. Amer. Meteor. Soc.*, **95**, 585–601, https://doi.org/10.1175/BAMS-D-12-00050.1.

Kumar, A., and M. P. Hoerling, 1998: Annual cycle of Pacific–North American seasonal predictability associated with different phases of ENSO. *J. Climate*, **11**, 3295–3308, https://doi.org/10.1175/1520-0442(1998)011<3295:ACOPNA>2.0.CO;2.

Lemos, M. C., 2008: What influences innovation adoption by water managers? Climate information use in Brazil and the United States. *J. Amer. Water Resour. Assoc.*, **44**, 1388–1396, https://doi.org/10.1111/j.1752-1688.2008.00231.x.

Marbaix, P., H. Gallee, O. Brasseur, and J.-P. van Ypersele, 2003: Lateral boundary conditions in regional climate models: A detailed study of the relaxation procedure. *Mon. Wea. Rev.*, **131**, 461–479, https://doi.org/10.1175/1520-0493(2003)131<0461:LBCIRC>2.0.CO;2.

Misra, V., 2006: Addressing the issue of systematic errors in a regional climate model. *J. Climate*, **20**, 801–818, https://doi.org/10.1175/JCLI4037.1.

——, 2020: *Regionalizing Global Climate Variations: A Study of the Southeastern U.S. Regional Climate.* Elsevier, 324 pp.

——, and A. Bhardwaj, 2020: Understanding the seasonal variation of Peninsular Florida. *Climate Dyn.*, **54**, 1873–1885, https://doi.org/10.1007/s00382-019-05091-7.

——, S. DiNapoli, and S. Bastola, 2012: Dynamic downscaling of the twentieth-century reanalysis over the southeastern United States. *Reg. Environ. Change*, **13**, 15–23, https://doi.org/10.1007/s10113-012-0372-8.

——, H. Li, Z. Wu, and S. DiNapoli, 2013: Global seasonal climate predictability in a two-tiered forecast system. Part I: Boreal summer and fall seasons. *Climate Dyn.*, **42**, 1425–1448, https://doi.org/10.1007/s00382-013-1812-y.

——, C. Selman, A. J. Waite, S. Bastola, and A. Mishra, 2017: Terrestrial and ocean climate of the 20th century. *Florida's Climate: Changes, Variations, and Impacts*, E. P. Chassignet et al., Eds., Florida Climate Institute, 330–389.

——, A. Mishra, A. Bhardwaj, K. Viswanathan, and D. Schmutz, 2018: The potential role of land cover on secular changes of the hydroclimate of Peninsular Florida. *npj Climate Atmos. Sci.*, **1**, 5, https://doi.org/10.1038/s41612-018-0016-x.

——, ——, and ——, 2019: A coupled ocean-atmosphere downscaled climate projection for the peninsular Florida region. *J. Mar. Syst.*, **194**, 25–40, https://doi.org/10.1016/j.jmarsys.2019.02.010.

——, T. Irani, L. Staal, K. Morris, T. Asefa, C. Martinez, and W. Graham, 2021: The Florida Water and Climate Alliance (FloridaWCA): Developing a stakeholder-scientist partnership to create actionable science in climate adaptation and water resource management. *Bull. Amer. Meteor. Soc.*, **102**, E367–E382, https://doi.org/10.1175/BAMS-D-19-0302.1.

Moorthi, S., and M. J. Suarez, 1992: Relaxed Arakawa–Schubert. A parameterization of moist convection for general circulation models. *Mon. Wea. Rev.*, **120**, 978–1002, https://doi.org/10.1175/1520-0493(1992)120<0978:RASAPO>2.0.CO;2.

Nag, B., V. Misra, and S. Bastola, 2014: Validating ENSO teleconnections on Southeastern United States winter hydrology. *Earth Interact.*, **18**, https://doi.org/10.1175/EI-D-14-0007.1.

Palmer, T. N., 2002: The economic value of ensemble forecasts as a tool for risk assessment: From days to decades. *Quart. J. Roy. Meteor. Soc.*, **128**, 747–774, https://doi.org/10.1256/0035900021643593.

——, Č. Branković, and D. Richardson, 2000: A probability and decision-model analysis of PROVOST seasonal multimodel ensemble integrations. *Quart. J. Roy. Meteor. Soc.*, **126**, 2013–2033, https://doi.org/10.1256/smsqj.56702.

Rayner, N. A., D. E. Parker, E. B. Horton, C. K. Folland, L. V. Alexander, D. P. Rowell, E. C. Kent, and A. Kaplan, 2003: Global analyses of sea surface temperature, sea ice, and night marine air temperature since the late nineteenth century. *J. Geophys. Res.*, **108**, 4407, https://doi.org/10.1029/2002JD002670.

Richardson, D. S., 2000: Skill and relative economic value of the ECMWF ensemble prediction system. *Quart. J. Roy. Meteor. Soc.*, **126**, 649–667, https://doi.org/10.1002/qj.49712656313.

——, 2006: Predictability and economic value. *Predictability of Weather and Climate*, T. Palmer and R. Hagedorn, Eds., Cambridge University Press, 628–644.

Shi, S., and V. Misra, 2020: The role of extreme rain events in Peninsular Florida's seasonal hydroclimate variations. *J. Hydrol.*, **589**, 125182, https://doi.org/10.1016/j.jhydrol.2020.125182.

Slingo, J. M., 1987: The development and verification of a cloud prediction model for the ECMWF model. *Quart. J. Roy. Meteor. Soc.*, **113**, 899–927, https://doi.org/10.1002/qj.49711347710.

Stefanova, L., V. Misra, S. Chan, J. J. O'Brien, and T. J. Smith III, 2012: A proxy for high resolution regional reanalysis for the Southeast United States: Assessment of precipitation variability. *Climate Dyn.*, **38**, 2449–2466, https://doi.org/10.1007/s00382-011-1230-y.

Tapiador, F. J., R. Roca, A. Del Genio, B. DeWitte, W. Petersen, and F. Zhang, 2019: Is precipitation a good metric for model performance? *Bull. Amer. Meteor. Soc.*, **100**, 223–233, https://doi.org/10.1175/BAMS-D-17-0218.1.

Tiedtke, M., 1983: The sensitivity of the time-mean large-scale flow to cumulus convection in the ECMWF model. *Proc. ECMWF Workshop on Convective in Large-Scale Models*, Reading, United Kingdom, European Centre for Medium-Range Weather Forecasts, 297–316.

Tuttle, S., and G. Salvucci, 2016: Empirical evidence of contrasting soil moisture–precipitation feedbacks across the United States. *Science*, **352**, 825–828, https://doi.org/10.1126/science.aaa7185.

Warner, T. T., R. A. Peterson, and R. E. Treadon, 1997: A tutorial on lateral boundary conditions as a basic and potentially serious limitation to regional numerical weather prediction. *Bull. Amer. Meteor. Soc.*, **78**, 2599–2617, https://doi.org/10.1175/1520-0477(1997)078<2599:ATOLBC>2.0.CO;2.

Whateley, S., R. N. Palmer, and C. Brown, 2015: Seasonal hydroclimatic forecasts as innovations and the challenges of adoption by water managers. *J. Water Resour. Plann. Manage.*, **141**, https://doi.org/10.1061/(ASCE)WR.1943-5452.0000466.

Yang, S., and E. A. Smith, 2008: Convective-stratiform precipitation variability at seasonal scale from 8 Yr of TRMM observations: Implications for multiple modes of diurnal variability. *J. Climate*, **21**, 4087–4114, https://doi.org/10.1175/2008JCLI2096.1.

Zhang, G. J., and N. A. McFarlane, 1995: Sensitivity of climate simulations to the parameterization of cumulus convection in the Canadian Climate Centre general circulation model. *Atmos. Ocean*, **33**, 407–446, https://doi.org/10.1080/07055900.1995.9649539.

Zhao, Q., and F. H. Carr, 1997: A prognostic cloud scheme for operational NWP models. *Mon. Wea. Rev.*, **125**, 1931–1953, https://doi.org/10.1175/1520-0493(1997)125<1931:APCSFO>2.0.CO;2.